Journal of Alloys and Compounds 509 (2011) 9284–9288

Contents lists available at ScienceDirect

Journal of Alloys and Compounds

journal homepage: www.elsevier.com/locate/jallcom

Electronic structure of antiferromagnetic $PbCrO_3$ (0 0 1) surfaces

Hasan Yıldırım*, Savaş Ağduk, Gökhan Gökoğlu

Department of Physics, Karabük University, 78050 Karabük, Turkey

ARTICLE INFO

Article history:
Received 8 April 2011
Received in revised form 7 June 2011
Accepted 22 June 2011
Available online 29 June 2011

Keywords:
Oxide materials
Atomic scale structure
Electronic properties
Computer simulations

ABSTRACT

Surfaces of cubic perovksite $PbCrO_3$ in (0 0 1) plane are investigated through density functional theory. The plane wave pseudopotential method is applied with generalized gradient approximation scheme. Hubbard U correction (GGA + U) is included in all calculations in order to simulate on-site Coulomb interactions between Cr–d states. Two types of terminations, namely, PbO- and CrO_2-terminations are considered in construction of the surfaces. Surfaces of both terminations show convergence at 9-layer slab geometry. The density of states calculations on the converged slab geometry yield a metallic behavior for both PbO- and CrO_2-terminations. Both metal atoms, Pb and Cr, in the uppermost layer of the respective terminations, have inward atomic relaxations much larger in magnitude than the oxygen atoms of the respective layer. However, Cr atoms which are labeled as up and down according to their spin orientation show different relaxations. The interlayer distance between the uppermost layer and the first one next to it decreases in both PbO- and CrO_2-terminated surface geometries. The calculations of the relative movement of the oxygen atom with respect to the Pb or Cr atom in each terminations give a positive rumpling in the uppermost layer.

1. Introduction

Cubic perovskites of transition metal oxides, ABO_3 in which A is a larger size cation in 12-coordination with oxygens, while B is a smaller cation in 6-coordination with oxygens, have very interesting properties like ferro-magnetism, ferro-electricity, and multiferroism owing to their 3d electrons in the partially filled B site [1]. Among the group, several chromites (e.g. $PbCrO_3$, $CaCrO_3$ and $SrCrO_3$) have attracted little interest although they have a rich variety of electronic and magnetic properties [2]. This is due to the difficulties in the production process such as requirement of high pressures and temperatures [2]. Even though the conditions are met, pure $PbCrO_3$ is barely synthesizable [2]. $PbCrO_3$ was first produced under high pressure and at high temperatures by Roth and DeVries [3]. The experiments at room temperature showed that $PbCrO_3$ is in cubic structure with a lattice constant of about ≈4.0 Å [3–5]. Experiments put out that $PbCrO_3$ is a semiconductor and exhibits antiferromagnetism with a magnetic moment of about 1.9 μ_B per Cr ion [5]. In recent years, cubic perovskite $PbCrO_3$ has been in the focus of several experimental works [1,2,6,7]. According to the experiments, $PbCrO_3$ actually had a lead deficiency described by $Pb_{1-x}CrO_{3-x}$ which caused a kind of modulated structure [6]. On the other hand, a spin reorientation was observed as a function of time in $PbCrO_3$ but further confirmations are required by means of neutron diffraction experiments [7]. A large volume collapse in the isostructural transition of $PbCrO_3$ from phase I to phase II at about 1.6 GPa was observed in a very recent experiment [1]. Although, the number of experimental studies on $PbCrO_3$ are increasing, there are few theoretical calculations [1,2,8] concerning the electronic band structure and magnetic properties.

Perovksite surfaces have many applications in technologically important areas ranging from sensors, photocatalysis, solid oxide fuel cells, steam electrolysis, actuators, capacitors to charge storage devices. For further developments in such applications, a better understanding of the surface structure of the perovskites and their related electronic properties are essential. Although some cubic perovksite surfaces such as $PbZrO_3$, $SrZrO_3$, $PbTiO_3$, and $BaMnO_3$ [9–13] have been under intense investigations both in theoretical and experimental aspects, $PbCrO_3$ surfaces have not been studied up to date. In view of all the applications aforementioned, structural and electronic properties of the lead chromite surfaces should be addressed. Therefore, we have systematically investigated structural and electronic properties of relaxed cubic perovskite $PbCrO_3$ (0 0 1) surfaces using DFT + U methods.

The rest of the paper is organized as follows: The details of computational methods and numerical parameters used in calculations are given in Section 2. Bulk structure of cubic $E2_1$ phase and its (0 0 1) surfaces with two different terminations are discussed in Section 3. Then paper concludes with a summary in Section 4.

2. Computational details

All the calculations presented in this work have been carried out using the PWscf code, distributed with the Quantum ESPRESSO

* Corresponding author. Tel.: +90 370 433 8374; fax: +90 370 433 8334.
E-mail address: hasanyildirim@karabuk.edu.tr (H. Yıldırım).

0925-8388/$ – see front matter © 2011 Elsevier B.V. All rights reserved.
doi:10.1016/j.jallcom.2011.06.096

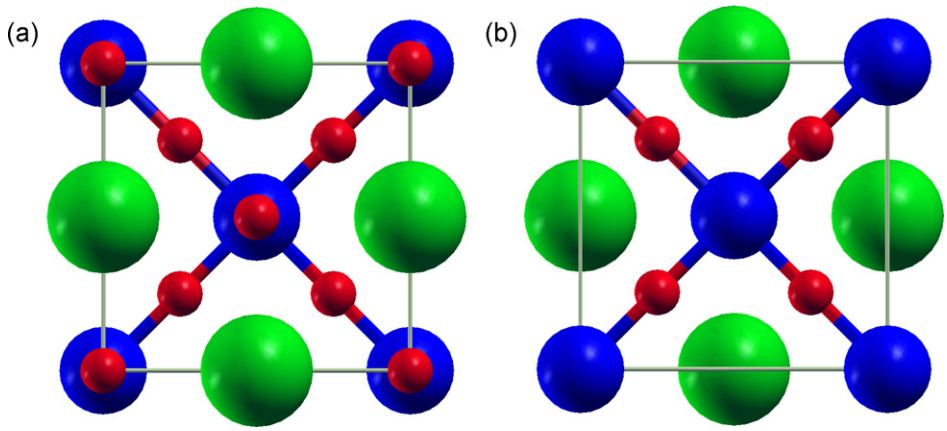

Fig. 1. Top views of (a) PbO- and (b) CrO_2-terminated (0 0 1) surfaces. Blue, green, and red balls represent the Cr, Pb, and O atoms, respectively.

package [14,15]. The exchange-correlation potential is approximated by spin-polarized generalized gradient approximation of the density functional theory [16,17] with Perdew–Burke–Ernzerhof parametrization [18]. Ultrasoft pseudopotentials (USPP) generated by Vanderbilt code [19] are used for all the atoms in composition. A scalar relativistic calculation scheme is followed for all the atoms with non-linear core correction. The valence states of the atoms are; Pb: $5d^{10}\ 6s^2\ 6p^2$, Cr: $3s^2\ 3p^6\ 4s^1\ 3d^5$, and O: $2s^2\ 2p^4$. For the case of chromium, $3s^2\ 3p^6$ states are treated as semi-core.

The crystal structure of cubic $PbCrO_3$ conforms to $E2_1$ symmetry with $Pm\bar{3}m$ space group. In order to describe G-type anti-ferromagnetic structure, we use a tetragonal supercell as explained in next section. Brillouin zone integration is performed with automatically generated $7 \times 7 \times 5$ k-point mesh yielding 228 k-points centered at Γ-point following the convention of Monkhorst and Pack [20]. Wave-functions are expanded in plane wave basis sets up to a kinetic energy cut-off value of 80 Ry. This corresponds to the approximately 9300 plane waves. These values are determined by testing convergence in self-consistent calculations. Davidson type iterative diagonalization method [21] is used in order to solve Kohn–Sham equations with 1×10^{-7} Ry energy convergence threshold. A Methfessel-Paxton type smearing is applied on fermionic occupation function with 0.001 Ry smearing parameter in order to accelerate electronic convergence via increasing electron temperature.

Local spin density approximation (LSDA) and generalized gradient approximation (GGA) functionals fail to describe strongly correlated electron systems with localized d and f orbitals. This is mostly encountered in transition metal oxides. In such a case, the on-site Coulomb interaction with an effective Hubbard U parameter (DFT + U) is included. The on-site Coulomb (U) and exchange (J) parameters are not separately taken into account in the approach of Dudarev et al. [22], but the difference $U-J$ which is physically meaningful is applied. Then the additional term due to interactions of the strongly correlated Cr–3d electrons is in the following form:

$$E(\mathrm{GGA}+U) = E(\mathrm{GGA}) + \frac{U-J}{2}\sum_{\sigma}\left[Tr\rho^{\sigma} - Tr(\rho^{\sigma}\rho^{\sigma})\right]. \quad (1)$$

In the equation above, ρ is the density matrix of Cr–3d states having spin σ. Hereafter, we call the difference $(U-J)$ as a single parameter U_{eff}.

In investigation of surface properties, we consider both PbO- and CrO_2-terminated (0 0 1) surfaces using slab geometry within a tetragonal cell. The top view of the each termination is shown on panels of (a) and (b) in Fig. 1. The blue, green, and red balls stand for Cr, Pb, and O atoms, respectively. 5, 7, and 9-layer surfaces are simulated in order to determine the convergence. All slabs modeled are symmetrically terminated. The central layers are fixed while the rest of layers are allowed to relax in each geometry. The slabs are repeated in z-direction with ∼15 Å vacuum distance. The surface structures are treated as in G-type antiferromagnetic order. Brillouin zone integration is realized with $5 \times 5 \times 1$ k-point grid. The structure optimization process is performed by Broyden–Fletcher–Goldfarb–Shanno (BFGS) algorithm [23]. The ionic minimization is carried out until the forces on the atoms are less than 1×10^{-4} Ry/a.u. and the displacement of the atoms are converged to less than 0.003 a.u.

3. Results and discussion

Firstly, we have checked the ground state structure of bulk $PbCrO_3$ in perovskite structure for different magnetic orders. The ferromagnetic (FM), G-type antiferromagnetic (G-AFM), and non-magnetic (NM) states have been simulated and the ground state total energies at equilibrium have been determined. According to these calculations, the equilibrium energy of G-type antiferromagnetic structure per formula unit of $PbCrO_3$ is ≈1 mRy and ≈62 mRy lower than the ferromagnetic and and non-magnetic states, respectively. This situation indicates the G-type antiferromagnetic structure as energetically favorable magnetic state at zero pressure as already verified by the earlier experimental measurements [3,5]. G-type antiferromagnetic ordering of spins is realized by antiparallel alignment of nearest neighbors, while next-nearest neighbors are in parallel orientation as shown in Fig. 2. In order to accommodate G-type antiferromagnetic structure, we use a body-centered tetragonal supercell containing two formula unit of atoms (10 atoms) with $\sqrt{2}a_0 \times \sqrt{2}a_0 \times 2a_0$, where a_0 is the lattice constant of initial cubic cell of perovskite structure ($E2_1$, $pm\bar{3}m$ space group). The on-site Coulomb interaction is also included with introducing Hubbard-U_{eff} parameter in the range 0–6 eV. This interaction is specially important for localized d-electronic states of chromium atom which is in the 4+ valence state. We construct the static equation of states of the bulk structure of $PbCrO_3$ using Vinet formulation [24] for various U_{eff} parameters and the results of equilibrium structural parameters are presented in Table 1. Since the U_{eff} is a priori unknown parameter, we are able to adjust it to reproduce the experimental values of structural parameters. It is clearly seen that the equilibrium lattice constant is slightly dependent on the U_{eff} parameter and the experimental value $a_0 = 4.0132$ Å [1] can not be achieved even at the very high values of U_{eff}. The increase of U_{eff} parameter leads a monotonic increase in saturation magnetic moment and equilibrium lattice constant. The bulk modulus is gradually decreased from 165.3 GPa to 137.7 GPa following the expansion of the lattice for U_{eff} between 2 eV and 6 eV. In this sit-

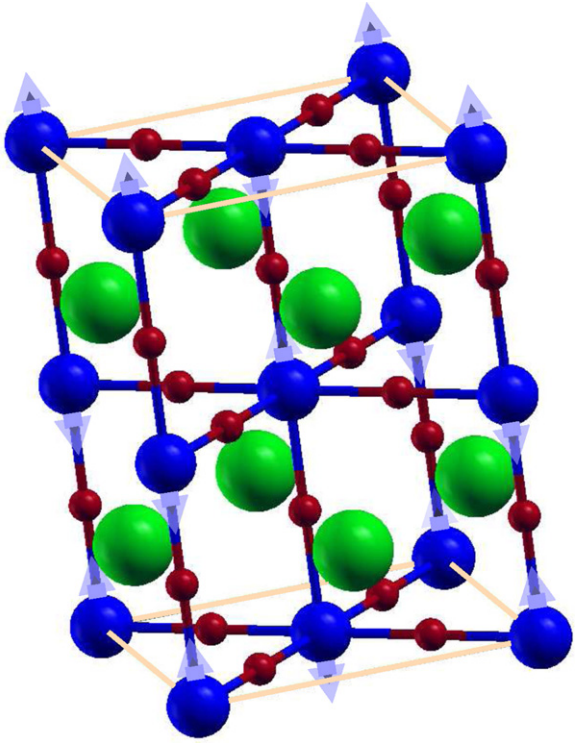

Fig. 2. G-type antiferromagnetic superstructure of $PbCrO_3$. Blue, green, and red balls represent the Cr, Pb, and O atoms, respectively.

uation, it seems to be more reasonable to optimize U_{eff} giving a magnetic moment as much as close to experimentally observed value which is ~2.51 μ_B for each chromium atom [7]. Then the optimized U_{eff} parameter happens to be 2.5 eV delivering a 2.52 μ_B magnetic moment. The bulk modulus for U_{eff} = 2.5 eV is 162.3 GPa which is consistent with the 187 GPa experimental value [1]. The optimized U_{eff} value then will be used in further calculations.

We display the orbital projected electronic density of states of bulk $PbCrO_3$ in Fig. 3(a). The total densities of states for up and down states of the material are exactly same as a consequence of the antiferromagnetic spin alignment of magnetic chromium atom. There are two chromium atom in primitive cell of G-type AFM structure, majority (up) spin density of 1st Cr atom is same with the minority (down) spin density of 2nd Cr atom (or vice versa). In this situation, up and down states of chromium atom can be given as spin polarized. The electronic behavior of the compound is mainly determined by the d-states of chromium atom. As clearly seen, the system exhibit strong metallic character with Cr–d and O–p bands crossing the Fermi level. The electronic states of Pb lie ~4 eV above the Fermi energy. The ground state electronic structure of the system under study has been reported as semiconducting antiferromagnet in earlier [5] and recent [7] experimental studies. Our calculations do not indicate a semiconducting behavior within the U_{eff} = 0–6 eV range. Moreover, NM and FM structures are also metallic. We check the stability of electronic structure up

Table 1
Equilibrium structural parameters of $PbCrO_3$ for various U_{eff} parameters.

U_{eff} (eV)	μ (μ_B)	a_0 (Å)	B (GPa)	B'
2	2.43	3.879	165.3	5.57
2.5	2.52	3.883	162.3	5.62
3	2.62	3.888	159.1	5.68
4	2.80	3.898	152.4	5.77
5	2.94	3.910	145.3	5.88
6	3.10	3.923	137.7	6.10

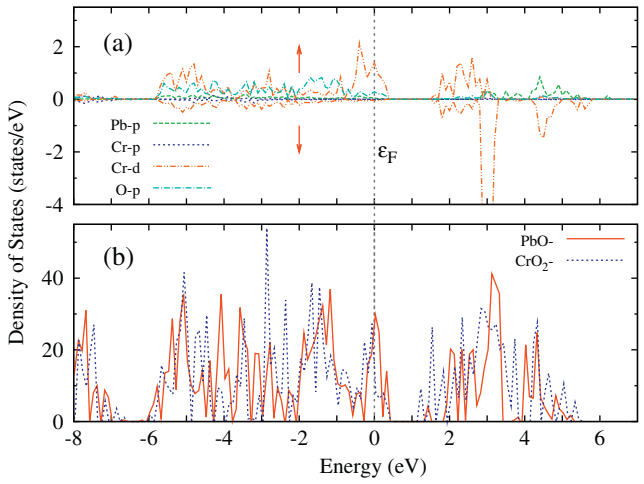

Fig. 3. Electronic density of states of (a): orbital projected for bulk $PbCrO_3$ and (b): total for PbO- and CrO_2-terminated (0 0 1) surfaces.

to 15 GPa pressure. Under these conditions, the general characteristics of electronic structure of the system are still preserved manifesting metallic band structure with only an upward shift of the Fermi level. The controversy of experimental and theoretical results can be attributed to the presence of impurities such as nonmagnetic PbO and Pb_5CrO_8 and antiferromagnetic Cr_2O_3 up to 10% [7]. The non-collinear magnetic states can also be present in magnetic structure.

The surface energy is a key parameter for determination of the well-converged surface structure. The average surface energy is given by the relation;

$$E_{surf} = \frac{1}{4}\left(E_{slab}^{PbO} + E_{slab}^{CrO_2} - NE_{bulk}\right) \quad (2)$$

where E_{slab}^{PbO} ($E_{slab}^{CrO_2}$) is the total energy of PbO- (CrO_2-) terminated surface, E_{bulk} is the energy of the bulk $E2_1$ perovskite structure, N is the number of layers. The average surface energies of 5, 7, and 9-layer surfaces are calculated as 46.69 mRy, 45.00 mRy, and 44.49 mRy, respectively. According to these energy values, it is clear that 9-layer slab is a sufficiently converged geometry. In Ref. [25], it is suggested that 7-layer slab provides convergence and 8- and 9-layer slabs do not bring any considerable changes in structural properties (less than 0.2%) of $PbTiO_3$, $BaTiO_3$, and $SrTiO_3$ cubic perovskite systems. However, we use 9-layer slab in order to investigate the electronic and structural properties of $PbCrO_3$ (0 0 1) surfaces due to the convergence. The 9-layer slabs contain 44(46) atoms for PbO-(CrO_2-) terminated surfaces. In this geometry, PbO-terminated slab is composed of five PbO and four CrO_2 layers, while CrO_2-terminated slab contains five CrO_2 and four PbO layers.

The total electronic density of states of PbO- and CrO_2-terminated surfaces are shown in Fig. 3(b). The structure of electronic states indicate a metallic behavior for both terminations. This is an expected situation, since the bulk structure is also found to be metallic. When the CrO_2-terminated surface is concerned, magnetic moments of up and down Cr atoms at uppermost layer are 1.88 μ_B and −2.63 μ_B, respectively. This situation indicates a disrupted antiferromagnetic behavior at surfaces. The magnetic moments at inner layers approach to its bulk value.

The geometry of relaxed surfaces are best described in terms of atomic relaxation (δZ), rumpling, and change of interlayer distance. In Table 2, atomic relaxations are given for uppermost layer and next three layers beneath it. As a consequence of the G-type antiferromagnetic superstructure given in Fig. 2, each PbO (CrO_2) layer consists of two Pb and two O (two Cr and four O) atoms. We give the relaxation of only one kind of atom for each layer, since

Table 2
Atomic relaxations (relative to ideal atomic positions) of the PbO- and CrO_2-terminated (0 0 1) surfaces of $PbCrO_3$ in percent of the cubic lattice constant a_0 = 3.883 Å. 1st layer corresponds to the outermost layer, while central layer (5th) is fixed.

Layer	PbO-terminated	δZ	CrO_2-terminated	δZ
1st	Pb	−5.124	Cr(↑)	−1.814
	O	−1.639	Cr(↓)	−3.390
			O	−0.117
2nd	Cr(↑)	+1.462	Pb	+3.482
	Cr(↓)	+1.455	O	−0.221
	O	+2.666		
3rd	Pb	−2.278	Cr(↑)	−1.260
	O	+2.181	Cr(↓)	−0.277
			O	−0.931
4th	Cr(↑)	+0.231	Pb	+0.625
	Cr(↓)	+0.468	O	−0.372
	O	+1.236		

identical atoms show the same amount of relaxation in z-direction. However, chromium atoms are exception due to their antiferromagnetically aligned spins in CrO_2-terminated surfaces. Therefore, we show the relaxations of both chromium atoms in the table. In the uppermost layer of PbO-terminated surface, both Pb atoms and O atoms move inward (i.e. along the $-z$ direction) with respect to the fixed central layer. The amount of relaxation is −5.124 (−1.639) for Pb (O). In the next lower layer, Cr atoms and O atoms move outward, that is along the $+z$ direction. Note that up Cr atom has a slightly higher relaxation than the down Cr atom. Compared to the atoms in the uppermost layer, metal atoms here have smaller relaxation but the O atoms have larger relaxation in magnitude. As for the third layer from the top, Pb atoms and O atoms in here show different relaxation directions: while Pb atoms move inwards as in the uppermost layer, O atoms move outward contrary to the O atoms of the uppermost layer. Cr atoms and O atoms in the lowest layer show the same behavior as the atoms in the second layer but the relaxations in that layer lower. On right side of Table 2, relaxation of atoms in the CrO_2-terminated surface are listed. The up and down Cr atoms in the first layer (i.e. the uppermost layer), exhibit relaxations of −1.814 and −3.390, respectively, while O atoms have relaxations of −0.117. That is to say, all atoms in the first layer move towards to the fixed central layer. However, there is a significant difference between the relaxations of up and down Cr atoms. O atom in here shows quite less relaxation compared to the O atom in uppermost layer of the PbO-terminated surface. In the second layer, Pb atoms move outward while O atoms move inward but the relaxation of Pb atoms are quite higher in magnitude. In the next lower layer, up Cr and down Cr atoms have inward relaxations but up Cr relaxes more. O atoms in the same layer moves in $-z$ direction as Cr atoms. As for the lowest layer, Pb atoms and O atoms move different directions similar to the atoms in the second layer.

The change of interlayer distance, Δd_{ij} between the layers i and j, is the second important parameter next to the relaxation as mentioned above. Δd_{ij} is calculated [25] through $\Delta d = [\delta Z(\mathrm{M}) + \delta Z(\mathrm{O})]/2$, here M labels the metal atom (Pb or Cr). We show Δd_{ij} for uppermost four layer in Table 3. For both terminations, the first layer display the highest change in interlayer distance which is also revealed in larger relaxations of that layer given in Table 2. The rest of the layers exhibits decreasing and oscillatory behavior for Δd_{ij} towards the central fixed layer which is a common behavior observed in various kind of materials ranging from perovskites [25] to metals [26] and metal oxides [26,27]. The cleavage of the bulk material yielding a surface structure reduces the symmetry of the geometry. This will remove the part of the potential which is available when the bulk periodicity in the direction normal to the surface exists [27]. Naturally, the effects will be much more pronounced on

Table 3
Change of the interlayer distance Δd_{ij} and layer rumpling η_i (in percent of the cubic lattice constant a_0 = 3.883 Å) for the relaxed PbO- and CrO_2-terminated 9-layer surfaces of $PbCrO_3$.

	PbO-terminated	CrO_2-terminated
Δd_{12}	−5.242	−3.404
Δd_{23}	+1.911	+2.454
Δd_{34}	−0.694	−0.950
Δd_{45}	+0.644	+0.128
η_1	+3.485	+2.485
η_2	+1.206	−3.702
η_3	+4.459	−0.161
η_4	+0.887	−0.997

the outermost layer. However, the effects due to lack of the periodicity will be attenuated towards the inner layers. In the same table, the rumpling η_i for ith layer is also given. The rumpling, η_i for ith layer is obtained using the relation $\eta = [\delta Z(\mathrm{O}) - \delta Z(\mathrm{M})]$ [28,29] which can be stated as the displacement of oxygen relative to metal atom. The oxygen atoms show positive rumpling at the first layer of both terminations. In the lower layers of PbO-terminated surface, the rumpling has positive sign, while the rumpling is negative for those of CrO_2-terminated surface. According to polarization model of Verwey, the sign of rumpling in metal oxide surfaces should be positive [27,30]. However, inner layers give negative rumplings for CrO_2-terminated surface. There are also other studies reporting negative rumplings for XO (X = Ca, Sr, Ba) (1 0 0) surfaces [27]. The sign of rumpling in metal oxide surfaces is still a matter of debate in literature. In order to see the change of δZ, rumpling (η_1), and interlayer distance (Δd_{12}) as function of slab thickness, we plot these parameters for uppermost layer of each slab in Fig. 4. The atomic relaxations of atoms show increasing displacement towards to central layer with increasing slab thickness except chromium atom in spin-up orientation. The rumpling for uppermost layer becomes larger with thicker slabs for both terminations. However,

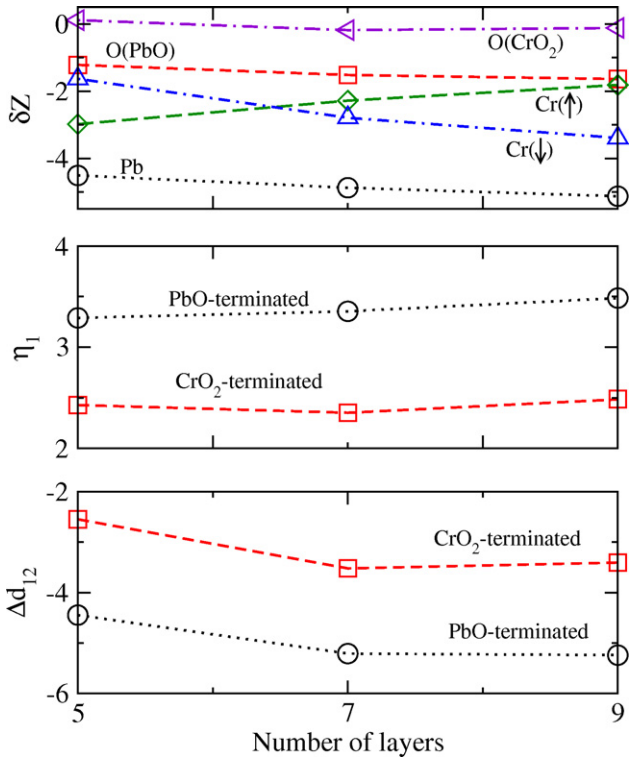

Fig. 4. Change of atomic relaxations δZ, rumpling (η_1), and interlayer distance (Δd_{12}) for outermost layer as a function of slab thickness.

the rumpling in PbO-terminated surface is always larger than that in CrO_2-terminated surface. The change of interlayer distance Δd_{12} in PbO-terminated surface is larger than that in CrO_2, which is mainly due to the large inward relaxation of Pb atom. Since the both surface terminations are charge neutral, there is not any surface reconstruction due to the absence of long range electric dipole moments.

4. Conclusion

In this study, we investigate the structural properties of (0 0 1) surfaces of cubic perovskite oxide $PbCrO_3$ by using spin-polarized GGA scheme of the density functional theory with Hubbard U correction. The system is treated as in G-type antiferromagnetic order which is the ground state magnetic phase of the related compound. The electronic behavior of the system is metallic for both bulk and surface structures within the range of U_{eff} considered. A symmetrically terminated slab model is used for investigation of the surface geometries with PbO- and CrO_2-terminations. Average surface energies are calculated for five, seven, and 9-layer slabs. The average energy of 9-layer surface indicate a well-converged surface structure. The rumpling of oxygen atoms are always positive for uppermost layers of both terminations indicating an outward movement relative to metal atom (Pb or Cr). The uppermost layers moves inward (towards the fixed central layer) during the ionic minimization for both terminations yielding a lower slab thickness.

The electronic conductivity measurements of the related compound indicate a semiconducting behavior as mentioned in previous experimental studies [5,7]. The our first principles calculations do not indicate a semiconducting behavior, even though the Hubbard U correction is included in calculation procedure. But as already explained in Ref. [7], the sample prepared contains nonmagnetic PbO and Pb_5CrO_8 and antiferromagnetic Cr_2O_3 impurities up to 10%. This may be a key point for electronic behavior of the system. Besides, the non-collinear magnetic states can also be present in magnetic structure.

Acknowledgements

This research was supported in part by TÜBİTAK (The Scientific & Technological Research Council of Turkey) through TR-Grid e-Infrastructure Project, part of the calculations have been carried out at ULAKBİM Computer Center.

References

[1] W. Xiao, D. Tan, X. Xiong, J. Liu, J. Xu, PNAS 107 (2010) 14026.
[2] A.M. Arévalo-López, E. Castillo-Martínez, M. Á Alario-Franco, J. Phys.: Condens. Matter 20 (2008) 505207.
[3] W.L. Roth, R.C. DeVries, J. Appl. Phys. 38 (1967) 951.
[4] R.C. DeVries, W.L. Roth, J. Am. Ceram. Soc. 51 (1968) 72.
[5] B.L. Chamberland, C.W. Moeller, J. Solid State Chem. 5 (1972) 39.
[6] A.M. Arévalo-López, M. Á Alario-Franco, J. Solid State Chem. 180 (2007) 3271.
[7] A.M. Arévalo-López, A.J. Dos santos-García, M. Á Alario-Franco, Inorg. Chem. 48 (2009) 5434.
[8] S.M. Jaya, R. Jagadish, R.S. Rao, R. Asokamani, Mod. Phys. Lett. B 6 (1992) 103.
[9] R.I. Eglitis, M. Rohlng, J. Phys.: Condens. Matter 22 (2010) 415901.
[10] Y.X. Wang, M. Arai, T. Sasaki, C.L. Wang, W.L. Zhong, Surf. Sci. 585 (2005) 75.
[11] G. Pilania, R. Ramprasad, Surf. Sci. 604 (2010) 1889.
[12] N. Li, K.L. Yao, G.Y. Gao, L. Zhu, Y.Y. Wu, J. Appl. Phys. 107 (2010) 123704.
[13] G. Gökoğlu, H. Yıldırım, Comput. Mater. Sci. 50 (2011) 1212.
[14] Quantum-ESPRESSO is a Community Project for High-quality Quantum-simulation Software, Based on Density-Functional Theory, and Coordinated by Paolo Giannozzi, <http://www.quantum-espresso.org> and <http://www.pwscf.org>.
[15] P. Giannozzi, S. Baroni, N. Bonini, M. Calandra, R. Car, C. Cavazzoni, D. Ceresoli, G.L. Chiarotti, M. Cococcioni, I. Dabo, A. Dal Corso, S. Fabris, G. Fratesi, S. de Gironcoli, R. Gebauer, U. Gerstmann, C. Gougoussis, A. Kokalj, M. Lazzeri, L. Martin-Samos, N. Marzari, F. Mauri, R. Mazzarello, S. Paolini, A. Pasquarello, L. Paulatto, C. Sbraccia, S. Scandolo, G. Sclauzero, A.P. Seitsonen, A. Smogunov, P. Umari, R.M. Wentzcovitch, J. Phys.: Condens. Matter 21 (2009) 395502.
[16] W. Kohn, L.J. Sham, Phys. Rev. 140 (1965) A1133.
[17] P. Hohenberg, W. Kohn, Phys. Rev. 136 (1964) B864.
[18] J.P. Perdew, K. Burke, M. Ernzerhof, Phys. Rev. Lett. 77 (1996) 3865.
[19] D. Vanderbilt, Phys. Rev. B 41 (1990) 7892 (Rapid communications).
[20] H.J. Monkhorst, J.D. Pack, Phys. Rev. B 13 (1976) 5188.
[21] E.R. Davidson, J. Comput. Phys. 17 (1975) 87.
[22] S.L. Dudarev, G.A. Botton, S.Y. Savrosov, C.J. Humphreys, A.P. Sutton, Phys. Rev. B 57 (1998) 1505.
[23] H.B. Schlegel, J. Comput. Chem. 3 (1982) 214.
[24] P. Vinet, J. Ferrante, J.R. Smith, J.H. Rose, J. Phys. C 19 (1986) L467.
[25] B. Meyer, J. Padilla, D. Vanderbilt, Faraday Discuss. 114 (1999) 395.
[26] J. Goniakowksi, C. Noguera, Surf. Sci. 323 (1995) 129.
[27] P. Broqvist, H. Grönbeck, I. Panas, Surf. Sci. 554 (2004) 262.
[28] J. Padilla, D. Vanderbilt, Phys. Rev. B 56 (1997) 1625.
[29] J. Padilla, D. Vanderbilt, Surf. Sci. 418 (1998) 64.
[30] E.J.W. Verwey, Recl. Trav. Chim. 65 (1946) 521.